Thermal video recording while walking: A simple method for mapping groundwater discharge points along forested headwater streams

Kenta Iwasaki[1], Keitaro Fukushima[2], Yu Nagasaka[3], Nobuo Ishiyama[3], Masaru Sakai[4], and Akiko Nagasaka[3]

[1]Forestry and Forest Products Research Institute
[2]Kyoto University
[3]Forestry Research Institute, Hokkaido Research Organization
[4]Fukushima Regional Collaborative Research Center, National Institute for Environmental Studies

November 23, 2022

Abstract

Groundwater discharge along channels can affect stream runoff, chemistry, and ecological communities. Although the spatial distribution of groundwater springs can be investigated by areal thermal remote sensing of wide rivers, this technique is difficult to apply to forested headwater streams because their channels are often covered by riparian trees. We present a method of mapping groundwater springs for forested headwater streams based on recording thermal video while walking along channels. We applied this method at two sites in Hokkaido, Japan. At one site, groundwater springs were spaced every ~100 m, and their distribution did not follow the topography at a 1.3-km-long reach underlain by Pleistocene andesite lava. Here, almost all of the springs were colder than stream water and had similar chemistries to each other. At the second site, cold and warm springs were underlain by Holocene volcanic ash. The cold springs mainly seeped from the streambed at the downstream part of the site while warm springs were located at the footslope. Some cold springs had much higher solute concentrations than the stream and warm springs, which suggests that the groundwater discharge to the stream had multiple sources. We also used our method to map the spatial heterogeneity of the stream temperature associated with groundwater inputs. This method is suitable for wide-area surveys because it can easily map the spatial distribution of the surface water temperature and the groundwater discharge along headwater streams.

Thermal video recording while walking: A simple method for mapping groundwater discharge points along forested headwater streams

Kenta Iwasaki[1,2*], Keitaro Fukushima[3,4], Yu Nagasaka[5], Nobuo Ishiyama[5], Masaru Sakai[6], and Akiko Nagasaka[5]

[1]Doto Station, Forestry Research Institute, Hokkaido Research Organization, Nishi5-sen 39-1, Shintoku, Hokkaido 081-0038, Japan.

[2]Present address: Center for Forest Damage and Risk Management, Forestry and Forest Products Research Institute, 1 Matsunosato, Tsukuba, Ibaraki 305-8687, Japan.

[3]Center for Ecological Research, Kyoto University, 2-509-3, Hirano, Otsu, Shiga, 520-2113, Japan

[4]Present address: Cluster of Agricultural Sciences, Faculty of Food and Agricultural Sciences, Fukushima University, 1 Kanayagawa, Fukushima, 960-1296, Japan

[5]Forestry Research Institute, Hokkaido Research Organization, Higashiyama, Koshunai, Bibai, Hokkaido 079-0198, Japan.

[6]Fukushima Regional Collaborative Research Center, National Institute for Environmental Studies, Japan, 10-2 Fukasaku, Miharu, Tamura District, Fukushima, 963-7700, Japan

*Corresponding author: Kenta Iwasaki (iwk@ffpri.affrc.go.jp)

Key Points:

- We present a quick and easy method to map groundwater discharge points in forested headwater streams using thermal video.
- Our method can map the spatial distribution of the surface water temperature and identify springs difficult to find with the naked eye.
- The water temperature map is useful for estimating sources of springs where multiple groundwater sources contribute to a stream.

Abstract

Groundwater discharge along channels can affect stream runoff, chemistry, and ecological communities. Although the spatial distribution of groundwater springs can be investigated by areal thermal remote sensing of wide rivers, this technique is difficult to apply to forested headwater streams because their channels are often covered by riparian trees. We present a method of mapping groundwater springs for forested headwater streams based on recording thermal video while walking along channels. We applied this method at two sites in Hokkaido, Japan. At one site, groundwater springs were spaced every ~100 m, and their distribution did not follow the topography at a 1.3-km-long reach underlain by Pleistocene andesite lava. Here, almost all of the springs were colder than stream water and had similar chemistries to each other. At the second site, cold and warm springs were underlain by Holocene volcanic ash. The cold springs mainly seeped from the streambed at the downstream part of the site while warm springs were located at the footslope. Some cold springs had much higher solute concentrations than the stream and warm springs, which suggests that the groundwater discharge to the stream had multiple sources. We also used our method to map the spatial heterogeneity of the stream temperature associated with groundwater inputs. This method is suitable for wide-area surveys because it can easily map the spatial distribution of the surface water temperature and the groundwater discharge along headwater streams.

1 Introduction

The variability of groundwater discharge along a river network is a critical scientific question that needs to be addressed to fill the scale gap between the headwater stream, downstream river, and deep groundwater flow (Wagener et al., 2021). Non-negligible amounts of water and solutes are lost through subsurface flow paths from the headwater catchment, and the deeply infiltrating groundwater usually discharges to downstream channels in basins with permeable geology (Asano et al., 2020; Egusa et al., 2016; Fan, 2019; Iwasaki et al., 2015). Thus, mapping the spatial variability of the groundwater discharge is key to understanding the changes in the stream runoff and chemistry from the headwater to downstream as well as the connectivity between local and regional groundwater systems.

Identifying the locations of groundwater discharge is also important with regard to the stream biota, water supply, and sediment disaster prevention. Groundwater discharge creates a suitable thermal habitat for aquatic organisms by modulating the temperatures of the stream and streambed (Briggs et al., 2013; Chu et al., 2008; Dugdale et al., 2013; Wilbur et al., 2020). Groundwater springs help increase biodiversity by creating unique environmental conditions (Meyer et al., 2007; Sakai et al., 2021). For humans, some villages utilize the discharge from groundwater springs as a water supply in not only dry regions (Nhu et al., 2020) but also humid regions (Ushijima et al., 2018). However, groundwater discharge can also be a potential pathway for contaminant transport (Thompson et al., 2021; Weatherill et al., 2014). Furthermore, searching for groundwater discharge zones may help with predicting the sites of potential deep-seated landslides (Jitousono et al., 2006). The multiple positive and negative functions of groundwater discharge suggest the importance of understanding the spatial distribution of upwelling water spots.

Thermal cameras are a popular method for identifying groundwater discharge zones, which have a different temperature from stream water. Although thermal cameras can only measure the water temperature at the surface, it is much less labor-intensive for surveys with a large spatial scale than direct observation using thermometers or fiber-optic distributed temperature sensing (FO-DTS). For surveys of wide rivers, groundwater discharge zones can be mapped by using a thermal camera mounted on an unmanned aerial vehicle (UAV), helicopter, or aircraft (Dugdale et al., 2022; Niwa, 2022; Rautio et al., 2015; Wilbur et al., 2020). However, this remote sensing technique is difficult to utilize for headwater streams because their channels and riverbanks are often covered by dense riparian trees.

Unlike the groundwater discharge from the outlet of zero-order hollows, springs from a bank or streambed are often difficult to find with the naked eye. Handheld thermal cameras are effective for detecting such springs in headwater streams (Barclay et al., 2022; Briggs et al., 2013; Redder et al., 2021; Roesky & Hayashi, 2022; Schuetz & Weiler, 2011). Mapping the presence-only data of detected springs does not confirm that no springs were overlooked. For wide-area surveys, an ideal approach is to automatically map the water temperature along the entire reach and obtain presence–absence data of the groundwater discharge. Hare et al. (2015) created a water temperature map by using a large dataset of photographs from a handheld thermal camera with Global Positioning System (GPS) data. They reported that the thermal camera identified patterns of groundwater seepage in smaller and shallow flowing streams, similar to FO-DTS. However, they also pointed out the disadvantages of the camera: the numerous thermal images are cumbersome for viewing the spatial configuration of a whole site, and human interpretation is required to remove the effects of objects other than water surface.

One potential solution to overcoming these inconveniences is video analysis. Thermal video can potentially be applied to mapping groundwater discharge zones with less trouble than thermal photographs because of the enormous amount of frame data in a single file. We present a method of using a handheld thermal video to create a water temperature map and identify groundwater discharge points along forested headwater streams. As a demonstration, we tested the proposed method in the summer at two sites in Hokkaido, Japan. The temperature map may also be useful for estimating sources of groundwater discharge because deeper groundwater has a more stable temperature than shallower groundwater. Thus, we analyzed the spring and stream water chemistry to examine if temperature of spring water is related to its sources.

2 Materials and Methods

2.1 Study sites

Figure 1 shows the study sites. The first survey was performed on August 26, 2020 at Site F (43°18′–19′ N, 142°37′–38′ E) in the University of Tokyo Hokkaido Forest, which is at Pon-nunobe River in Furano City. The bedrock mainly comprises Pleistocene andesite lava called Tairoku-san Lava, which is on older Tokachi Welded Tuff from the Pliocene to Pleistocene. This in turn covers Pre-Cretaceous sedimentary rock classified as the Hidaka Super Group (Osanai et al., 1968). Platy joints in the Tairoku-san Lava (Osanai et al., 1968) suggest that it is highly permeable. We surveyed a reach with an elevation of 744–851 m and drainage area of 289–583 ha. The surrounding vegetation was a mixed conifer–broadleaf forest. The Japan Meteorological Agency (JMA) has an Automated Meteorological Data Acquisition System (AMeDAS; https://www.jma.go.jp/jma/menu/menureport.html) station near Site F (Rokugou; 43°18.1′ N, 142°31.3′ E), and it recorded a mean annual temperature and precipitation of 6.3°C and 998 mm, respectively, for the 10-year period of 2012–2021. On the day of the survey, antecedent precipitation for the week and the mean daily temperature was 0.5 mm and 24.9°C, respectively.

The water temperature was recorded hourly during the observation period by using the Onset Hobo UA-001-171 at 5 km downstream of Site F (43°18.0′ N, 142°35.2′ E).

The second survey was conducted on July 17, 2021 at Site S (43°23′ N, 144°39′–40′E), which is in the Shibecha Branch of the Hokkaido Forest Research Station, Field Science Education and Research Center, Kyoto University. This is at Isochibetsu River in Shibecha Town. The geology of Site S comprises Quaternary Holocene volcanic ash that is called Mashu Volcanic Ash Layer I. We surveyed a reach with an elevation of 60–99 m and drainage area of 6–155 ha. The vegetation of the targeted watershed comprised a forest of natural broadleaf trees and partly planted conifers. In contrast, the neighboring watershed, which comprised the part of the volcanic ash plateau upstream of Site S, had pasture vegetation. The AMeDAS station near Site S (Shibecha; 43°17.5′ N, 144°35.2′ E), recorded a mean annual temperature and precipitation of 5.6°C and 1070 mm, respectively, for the past 10 years. On the day of the survey, antecedent precipitation for the week and the mean daily temperature were 1.5 mm and 22.3°C, respectively.

The surveys were conducted in the summer to maximize the temperature difference between the groundwater discharge and stream water. In addition, field surveys in the winter would have been difficult because of the snow cover and cold weather.

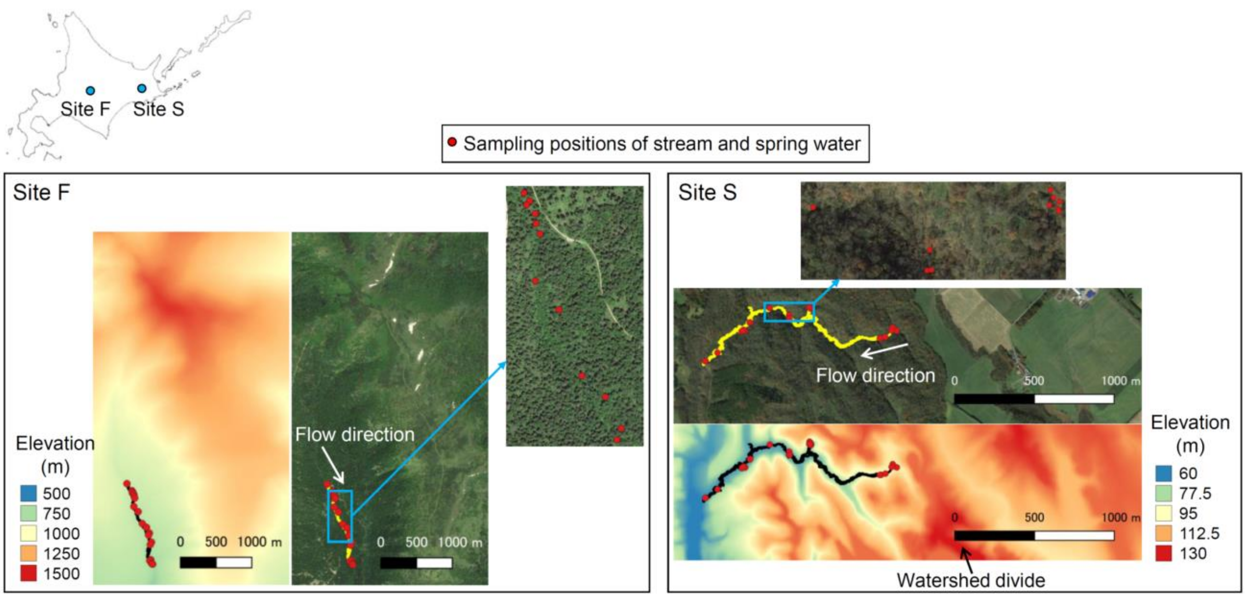

Figure 1. Elevation map and Google satellite imagery of the study sites (©2022 Google, CNES/Airbus, and Maxar Technologies). The elevation map was created from the Geospatial Information Authority of Japan’s 10 × 10-m digital elevation models (DEMs). Black and yellow lines indicate the GPS track.

2.2 Field survey

A thermal video of the water surface was shot while walking in the reaches and/or adjacent riparian zones of the study sites. The equipment is shown in Figure S1. Thermal images were obtained by using a compact thermal camera (FLIR C3, Flir Systems) that was connected to a tablet computer (Surface Go 2, Microsoft) with dedicated software (FLIR Tools+, Flir Systems). A waterproof case (PDA-TABWPST10BK, Sanwa Supply Inc.) was used to carry the tablet in the field. The times of the camera and tablet were calibrated before the surveys. The thermal video was recorded by using FLIR Tools+. The camera was worn on the chest using a neck strap and was pointed downward. Thus, the distance between the camera and water surface was maintained around 1–1.5 m. To obtain whole images of the reaches including both banks, we walked by turning our body at narrow channels. For wide channels, we walked in a zigzag pattern to approach both banks. We left the reaches and shot video from the riparian zones if there were obstacles such as fallen trees or cascades. Handy GPS (GPSmap 62sc, Garmin) was used to record the location information. The interval of the track log was set to auto-normal mode (approximately 20 s) at Site F. Because the interval was long, we stopped for several tens of seconds when we found an area with a different temperature from the surrounding stream water. At Site S, the interval was set to 5 s for the first ~30 min and 1 s after that.

Water samples were collected at various positions of mainstream, tributary, and groundwater springs found during the surveys. An inflow into the mainstream from a distinct channel with a drainage area of >1 ha was regarded as a tributary. Samples were collected in polyethylene bottles either directly or by using a syringe. Bottles and syringes were rinsed with sample water more than twice before sampling. The electrical conductivity (EC), pH, and water temperature were measured at all sampling points by using a portable meter (WM-32EP, CM-31P and HM-30P, DKK-TOA Corporation).

2.3 Data processing

The thermal video data were processed by using FLIR Tools+. The reflected temperature and stream surface emissivity are difficult to quantify. Thus, the empirical correction approach is useful for extracting the absolute stream temperature (Baker et al., 2019). Firstly, the tentative temperature was calculated by using 0.97 as the water emissivity and default values as the other parameters: a distance to object of 1 m; reflected temperature, atmospheric temperature, and external optical temperature of 20°C; external optical transmittivity of 1; and relative humidity of 50%. For each video file, the temporal changes in the minimum temperature within the full screen were plotted by using the Area tool and Plot tab of FLIR Tools+. If the water surface appeared on part of the screen, other objects (e.g., land surface and plants above water) did not affect the minimum temperature because they had a higher surface temperature than the stream and spring water (Figure S2). The plotted data were copied from FLIR Tools+ and were pasted into Microsoft Excel. By these processes, two or three minimum temperature data were obtained per second. The average value of consecutive three data was used as the minimum temperature for each second. Minimum-temperature data ranging between 0 and 20°C were regarded to represent the water temperature (Figure S3). Outlier data (>20 or <0°C) were recorded mostly when no water surface appeared on the screen or the camera was automatically calibrated.

Then, the temperature was corrected by using the following linear relationship empirically observed between the minimum tentative temperature recorded around the sampling point and actual water temperature from the portable meter (R^2 = 0.88; Figure S4):

$$T_A = 0.87 \times T_T + 3.4 \quad (1)$$

where T_A and T_T are the actual and tentative temperatures (°C), respectively. The observation points and timings of the tentative and actual temperatures slightly differed because we did not necessarily take a video of the same scene measured by the portable meter. However, the associated error should be negligible because we used data from many points (45 points).

Geographic information system (GIS) analysis was conducted by using QGIS 3.22.7. GPS track data were imported as point data by using the Batch GPS Importer plugin. The data were exported to a CSV file after geometry attributes were added. The water temperature data every second and GPS data were integrated by using Microsoft Excel. Then, the data of the water temperature and location of each time were saved as a CSV file and were imported to QGIS. The data were classified based on water temperature.

2.4 Chemical analysis

The samples were filtered through a GF/F filter with 0.63-μm pores in a laboratory. The samples were sealed in polyethylene bottles and were refrigerated at about 2°C until analysis. The Cl^-, NO_3^-, SO_4^{2-}, Na^+, K^+, Mg^{2+}, and Ca^{2+} concentrations were measured by using ion chromatography (Dionex ICS-1100; Thermo Fisher Scientific, Waltham, MA, USA). At Site S, The PO_4^{3-} concentration was also measured by using an auto-analyzer (QuAAtro 2-HR; BLTEC, Osaka, Japan).

2.5 Statistical analysis

Q-mode hierarchical cluster analysis (HCA) was conducted to classify the stream and spring water samples into hydrochemically similar groups, in accordance with Güler et al. (2002). The analysis was performed by using the EC, pH, and concentrations of all solute data and R 4.2.0 software (R Development Core and Team). Although Güler et al. (2002) log-transformed the data to more closely correspond to a normal distribution, we did not conduct a log transformation because most of the chemical variables were originally normally distributed (Shapiro–Wilk test, $p > 0.05$). All variables were standardized by calculating their standard scores (z-scores) using their means and standard deviations. The Euclidean distance (euclidean method in dist function) and Ward's method (ward.D2 method in hclust function) were used for the similarity measurement and linkage, respectively. The number of groups was selected based on visual examination of the dendrogram at each site. Differences in the chemical variables between groups were examined by the Tukey–Kramer test ($p < 0.05$).

3 Results

3.1 Spatial distribution of groundwater springs

At Site F, the water temperature was >11°C for the stream and <9°C for many groundwater springs (Figure 2a). The spatial heterogeneity in temperature was much greater than the fluctuations in the mainstream water temperature during the observation period (<0.6°C; Figure S5). Springs with a temperature of <9°C existed at 13 points in the 1.3-km reach. Most of the cold springs were not in the hollow with a concave topography. The thermal images enabled us to find springs gradually seeping from the flat streambank, which would be difficult to find by the naked eye (Figure S2).

At Site S, the spring distribution also did not follow the surface topography except for the spring from the hollow (near 12:00 in Figure 2b). Springs with a temperature of <9°C mainly upwelled from the streambed at the downstream part of Site S (Figure 2b). These springs were difficult to find without thermal images (Figure S2). There were also some warm springs with a temperature of >13°C. Although these springs were unclear in the thermal images, they were easily found with the naked eye because they trickled down from the footslope. Although the stream temperature was higher than 13°C in the upstream segment (upstream of 15:48 in Figure 2b), it decreased to 11–12°C in its downstream segment (downstream of 15:48) owing to the inflow of water from cold springs. The stream temperature declined to 10–11°C in the furthest downstream segment (downstream of 17:00). Because the stream temperature of the neighboring segments was observed at almost the same time, the difference between segments can be attributed to the mixture of springs and tributaries.

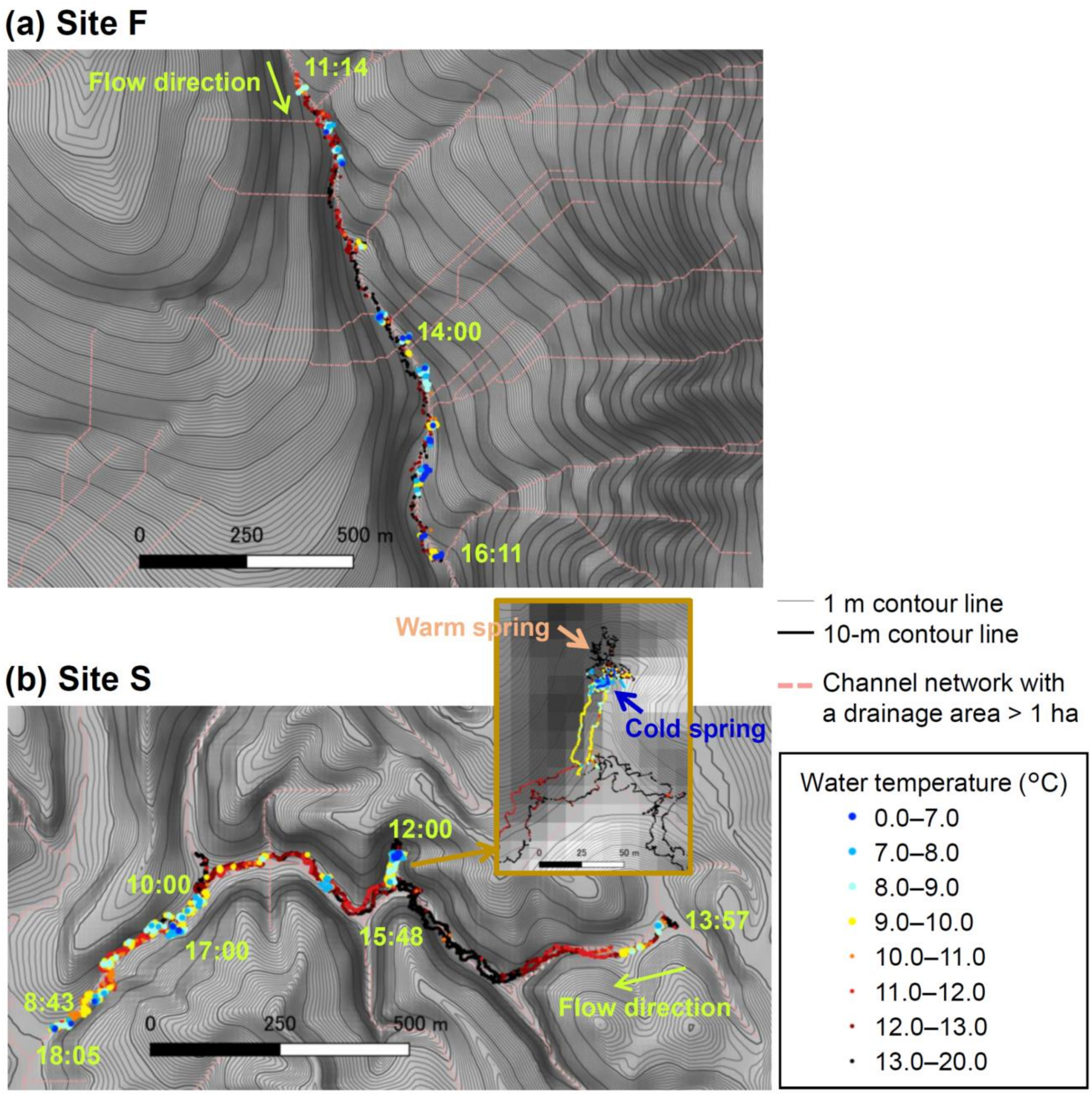

Figure 2. Water temperature maps generated from thermal video at (a) Site F and (b) Site S. The passage time on the track is also shown. One-way and round-trip surveys were conducted at Sites F and S, respectively.

3.2 Relationships between the water temperature and chemistry

At Site F, almost all springs had a lower temperature, higher EC, and higher concentrations of Na^{+}, Mg^{2+}, Ca^{2+}, and Cl^{-} than the mainstream (Figure 3a). In contrast, Site S had some springs with a higher temperature, lower EC, and lower concentrations of all solutes except for SO_4^{2-} than the mainstream (Figure 3b). Springs colder than the mainstream had greatly varying chemistry, and some had higher concentrations of all solutes than the mainstream and tributary water.

HCA showed the contrasting classification schemes between water samples from Sites F and S (Figure 4). Each site had three groups. At Site F, the springs and tributary (Groups 2 and 3) clearly had a different chemistry from the mainstream (Group 1) (Figure 4a). Groups 2 and 3 had a higher EC and concentrations of all solutes except for K^{+} and NO_3^{-} than Group 1 (Table S1). The difference in concentrations between Groups 2 and 3 was not significant for many solutes. The springs showed a similar water temperature but had different elevations between groups (Figures 4a and S6a; Table S2). At Site S, some springs were classified into the same group as the mainstream (Figure 4b). The EC and all solute concentrations except for SO_4^{2-} and PO_4^{3-} were significantly different between all groups. The clearest difference between groups was for the NO_3^{-} concentration, which was five times higher in Group 1 than in Group 2. Springs in Group 2 had a higher water temperature than the other groups despite being at a similar elevation (Figure S6b; Table S2).

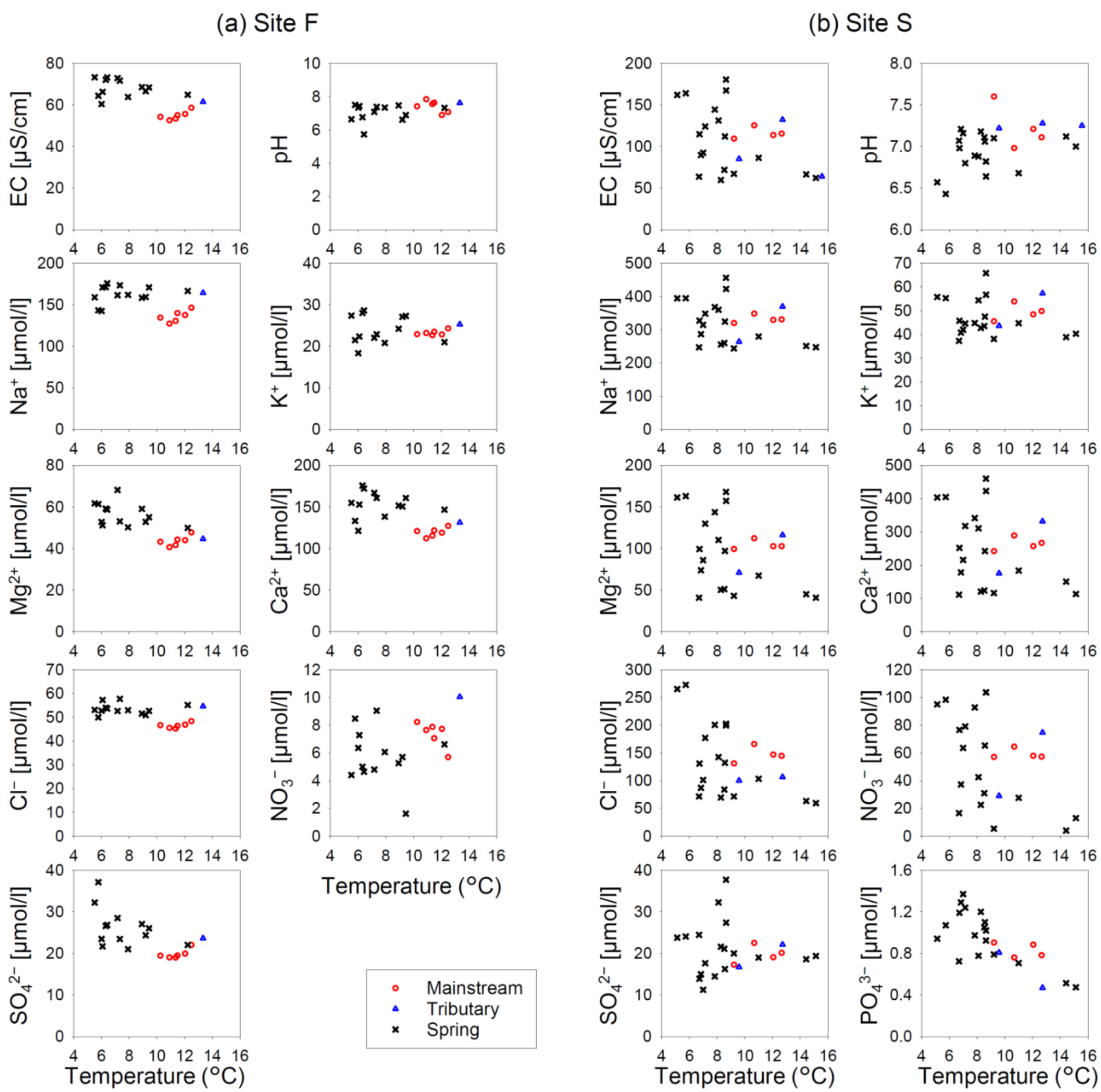

Figure 3. Relationships between the water temperature estimated from the thermal video and chemical variables: (a) Site F and (b) Site S.

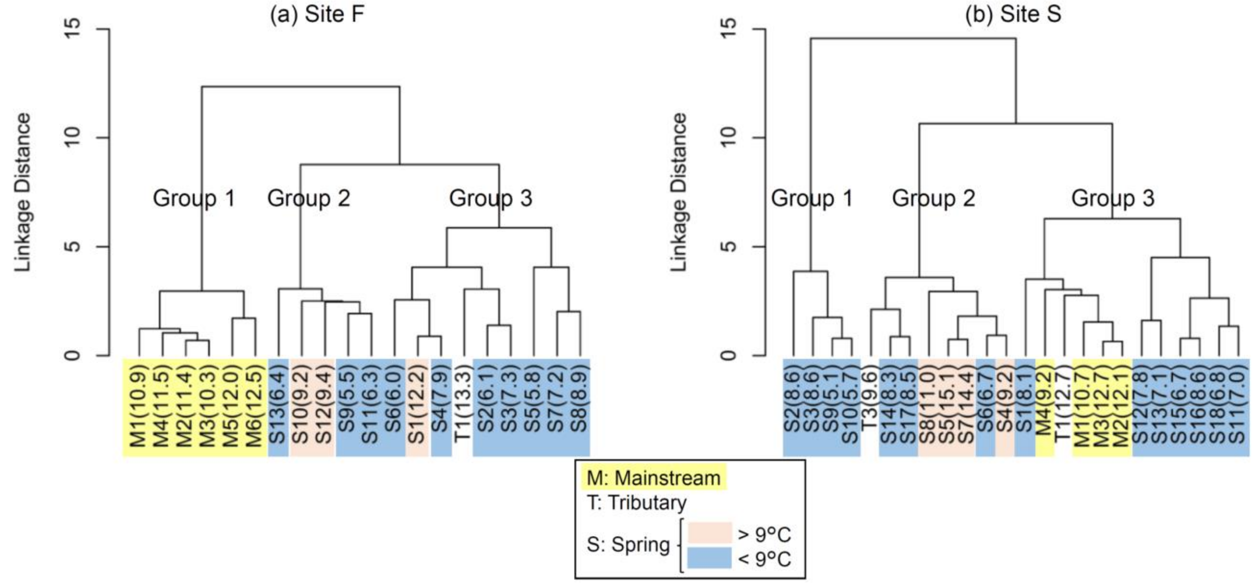

Figure 4. Dendrogram from HCA for the stream and spring water samples at (a) Site F and (b) Site S. The samples are numbered in descending order of elevation for each water category. The number in parentheses indicates the water temperature estimated from the thermal video.

4 Discussion

4.1 Merits of temperature mapping using thermal video

The spatial variability of the surface water temperature associated with the groundwater input could be mapped with a fine resolution even in forested headwater catchments, where aerial remote sensing is difficult to apply. The locations of cold groundwater discharges, which include seepage hard to find with the naked eye (Figure S2), could be clearly identified in the temperature map (Figure 2). Video recording does not require special skills, and a reach longer than 1 km could be surveyed in half a day each way. Moreover, unlike the analysis using thermal photographs (Hare et al., 2015), eliminating the effects of objects other than water required little effort because the minimum temperature of each frame can be automatically plotted. Although the observed temperature was underestimated, especially at low temperatures, it could be corrected by using a linear empirical relationship with the actual temperature (Figure S4). The underestimation can be attributed to our method of extracting the minimum temperature within the screen and the deviation of parameters as the object temperature decreased.

In contrast to the conventional method of simply mapping spring locations (i.e., presence-only data), our method can also map locations without springs (i.e., absence data) and the longitudinal spatial variation of stream temperature. The absence data are useful for confirming that nothing has been overlooked. Even if the survey is outsourced, our method ensures that all springs with characteristic temperatures are mapped. The spatial distribution of the stream temperature is also important information because of its complexity; it differs between segments (Brown & Hannah, 2008; Isaak et al., 2010; Kanno et al., 2014) and within a segment (Dzara et al., 2019) due to various factors such as the topography and different water sources. The spatiotemporal thermal heterogeneity would be higher in catchments with multiple geologies because the underlying geology also affects the groundwater discharge (Ishiyama et al., 2022; Tague et al., 2007). The behavior and distribution of stream organisms are closely linked to the spatiotemporal pattern of the water temperature. Thus, we believe that the information obtained by our method on the longitudinal thermal heterogeneity of headwaters will be valuable for future ecological research. For example, mapping the water temperature with our method can be a first step to finding suitable habitats for groundwater-dependent (crenobiont) species and thermal refuges from climate change.

4.2 Potential of temperature map for estimating sources of groundwater discharge

At Site S, cold springs had higher concentrations than warm springs of almost all solutes, especially NO_3^- (Figures 3 and 4). Stream water from a pasture has higher concentrations of many solutes including NO_3^- than that from a forested catchment due to fertilizer and excretion (Nakagawa et al., 2002; Woli et al., 2004), and such a pasture was adjacent to Site S. Nitrate contamination from agricultural areas has also been observed in groundwater, especially at catchments underlain by Quaternary volcanic ejecta in Hokkaido (Takada et al., 2009). Groundwater discharge can often be a source of NO_3^- in agricultural watersheds underlain by a permeable subsurface substrate (Redder et al., 2021; Richards et al., 2021). Considering the permeable geology and higher elevation of the neighboring pasture (Figure 1), our results suggests that inter-basin groundwater flow from the pasture contaminated the cold springs in Site S. In contrast, warm springs with diluted solutes may have discharged via a shallower local flow path from the targeted forested watershed. The coexistence of these different groundwater components (Figures 2 and S6) demonstrates the importance of mapping surface water temperature by field observations.

At Site F, the colder temperature and higher solute concentrations of the groundwater discharge (Figures 3 and 4) suggest that it had a deeper flow path than the stream water. This is consistent with the results of other Quaternary volcanic rock catchments where deeper groundwater contributed to stream water as the drainage area increased (Fujimoto et al., 2016). The similar spring chemistry between the two groups (Table S1) implies that all springs derived from a similar source, which caused an unclear relationship between the temperature and chemistry here. In contrast to Site F, multiple groundwater sources have been suggested to contribute to some volcanic catchments underlain by multiple lavas (Bertrand et al., 2010) and Neogene lava (Iwasaki et al., 2021). In such catchments, a water temperature map may be useful for distinguishing groundwater discharges from different sources, as was the case for Site S.

4.3 Limitations of the method

Although our method is quick and easy, it does have some limitations. First, the groundwater discharge from a deep water body may be hard to detect because our method observes the surface temperature. This is the same disadvantage of areal thermal remote sensing. However, Hare et al. (2015) pointed out that submerged seepage zones with a depth of <0.5 m can be identified clearly by using thermal cameras. Because our method is targeted towards headwater stream, which have shallow water depths, this disadvantage should not be significant. Second, the suitable observation time is limited. Our method is limited to the summer or winter, which have the largest differences in temperature between the stream water, groundwater discharge, and objects other than water. Our method is also less suitable for observing storm runoff because of the large temporal changes in water temperature during or just after rainfall. In addition, walking along the channels during these times may be dangerous. Finally, the precision of the spring location may be limited by the accuracy of portable GPS. Although we used consumer-grade GPS, the use of mapping-grade GPS or GNSS can improve the accuracy (Wing, 2008). For instance, Tokuni et al. (2016) showed near Site F that the mean and maximum positioning errors under the forest canopy were 2 and 4 m, respectively, for mapping-grade GNSS (Trimble Pro series 6H). In contrast, the mean and maximum positioning errors were 4 and 10–20 m, respectively, for consumer-grade GNSS (Garmin GPSMAP 62 SCJ), which was a similar model to ours.

Despite the above limitations, our method can be used to easily estimate the locations of groundwater discharge and the spatial distribution of the stream temperature in half a day along reaches of >1 km without requiring any special skills. Thus, our method will be useful for preliminary investigations before detailed observations and in wide-area surveys of groundwater inflows.

5 Conclusions

We presented a simple method for mapping groundwater discharge zones using thermal video. Its application at two sites demonstrated that springs could be successfully mapped even when they did not follow the characteristic topography. The proposed method obtains the presence–absence data of springs and the spatial distribution of the stream temperature. For sites where the groundwater derives from multiple sources, the water temperature map is useful for distinguishing groundwater discharges from different sources. Our method will be beneficial for wide-area surveys and preliminary investigations of groundwater dynamics in various fields and applications, including runoff processes, stream ecology, contaminant pathways, water supply, and landslide prediction.

Acknowledgments

Part of this study was supported by a grant from the 2020 Nippon Life Insurance Foundation and a strategic research grant from the Hokkaido Research Organization. We would like to thank the staffs of the University of Tokyo Hokkaido Forest and Hokkaido Forest Research Station of Kyoto University for their assistance with the field survey. We are also grateful to Dr. Ken Ushijima for the helpful discussions.

Open Research

All data used in the analysis are available from a repository (Iwasaki et al., 2022).

References

Asano, Y., Kawasaki, M., Saito, T., Haraguchi, R., Takatoku, K., Saiki, M., & Kimura, K. (2020). An increase in specific discharge with catchment area implies that bedrock infiltration feeds large rather than small mountain headwater streams. *Water Resources Research*, *56*(9), e2019WR025658. https://doi.org/10.1029/2019WR025658

Baker, E. A., Lautz, L. K., McKenzie, J. M., & Aubry-Wake, C. (2019). Improving the accuracy of time-lapse thermal infrared imaging for hydrologic applications. *Journal of Hydrology*, *571*, 60-70. https://doi.org/10.1016/j.jhydrol.2019.01.053

Barclay, J. R., Briggs, M. A., Moore, E. M., Starn, J. J., Hanson, A. E. H., & Helton, A. M. (2022). Where groundwater seeps: Evaluating modeled groundwater discharge patterns with thermal infrared surveys at the river-network scale. *Advances in Water Resources*, *160*, 104108. https://doi.org/10.1016/j.advwatres.2021.104108

Bertrand, G., Celle-Jeanton, H., Huneau, F., Loock, S., & Renac, C. (2010). Identification of different groundwater flowpaths within volcanic aquifers using natural tracers for the evaluation of the influence of lava flows morphology (Argnat basin, Chaîne des Puys, France). *Journal of Hydrology, 391*(3-4), 223-234. https://doi.org/10.1016/j.jhydrol.2010.07.021

Briggs, M. A., Voytek, E. B., Day-Lewis, F. D., Rosenberry, D. O., & Lane, J. W. (2013). Understanding Water Column and Streambed Thermal Refugia for Endangered Mussels in the Delaware River. *Environmental Science & Technology, 47*(20), 11423-11431. https://doi.org/10.1021/es4018893

Brown, L. E., & Hannah, D. M. (2008). Spatial heterogeneity of water temperature across an alpine river basin. *Hydrological Processes, 22*(7), 954-967. https://doi.org/10.1002/hyp.6982

Chu, C., Jones, N. E., Mandrak, N. E., Piggott, A. R., & Minns, C. K. (2008). The influence of air temperature, groundwater discharge, and climate change on the thermal diversity of stream fishes in southern Ontario watersheds. *Canadian Journal of Fisheries and Aquatic Sciences, 65*(2), 297-308. https://doi.org/10.1139/f08-007

Dugdale, S. J., Bergeron, N. E., & St-Hilaire, A. (2013). Temporal variability of thermal refuges and water temperature patterns in an Atlantic salmon river. *Remote Sensing of Environment, 136*, 358-373. https://doi.org/10.1016/j.rse.2013.05.018

Dugdale, S. J., Klaus, J., & Hannah, D. M. (2022). Looking to the Skies: Realising the Combined Potential of Drones and Thermal Infrared Imagery to Advance Hydrological Process Understanding in Headwaters. *Water Resources Research, 58*(2), e2021WR031168. https://doi.org/10.1029/2021WR031168

Dzara, J. R., Neilson, B. T., & Null, S. E. (2019). Quantifying thermal refugia connectivity by combining temperature modeling, distributed temperature sensing, and thermal infrared imaging. *Hydrology and Earth System Sciences, 23*(7), 2965-2982. https://doi.org/10.5194/hess-23-2965-2019

Egusa, T., Ohte, N., Oda, T., & Suzuki, M. (2016). Quantifying aggregation and change in runoff source in accordance with catchment area increase in a forested headwater catchment. *Hydrological Processes, 30*(22), 4125-4138. https://doi.org/10.1002/hyp.10916

Fan, Y. (2019). Are catchments leaky? *WIREs Water, 6*(6). https://doi.org/10.1002/wat2.1386

Fujimoto, M., Ohte, N., Kawasaki, M., Osaka, K., Itoh, M., Ohtsuka, I., & Itoh, M. (2016). Influence of bedrock groundwater on streamflow characteristics in a volcanic catchment. *Hydrological Processes, 30*(4), 558-572. https://doi.org/10.1002/hyp.10558

Güler, C., Thyne, G. D., McCray, J. E., & Turner, K. A. (2002). Evaluation of graphical and multivariate statistical methods for classification of water chemistry data. *Hydrogeology Journal, 10*(4), 455-474. https://doi.org/10.1007/s10040-002-0196-6

Hare, D. K., Briggs, M. A., Rosenberry, D. O., Boutt, D. F., & Lane, J. W. (2015). A comparison of thermal infrared to fiber-optic distributed temperature sensing for evaluation of groundwater discharge to surface water. *Journal of Hydrology, 530*, 153-166. https://doi.org/10.1016/j.jhydrol.2015.09.059

Isaak, D. J., Luce, C. H., Rieman, B. E., Nagel, D. E., Peterson, E. E., Horan, D. L., et al. (2010). Effects of climate change and wildfire on stream temperatures and salmonid thermal habitat in a mountain river network. *Ecological Applications, 20*(5), 1350-1371. https://doi.org/10.1890/09-0822.1

Ishiyama, N., Sueyoshi, M., Jorge, G. M., Iwasaki, K., Negishi, N. J., Koizumi, I., et al. (2022). The role of geology in creating stream climate-change refugia along climate gradients. *bioRxiv*. https://doi.org/10.1101/2022.05.02.490355

Iwasaki, K., Fukushima, K., Nagasaka, Y., Ishiyama, N., Sakai, M., & Nagasaka, A. (2022). *Data of thermal video surveys along forested headwater streams in Hokkaido, Japan [Dataset]*. Retrieved from: https://doi.org/10.6084/m9.figshare.20960455

Iwasaki, K., Katsuyama, M., & Tani, M. (2015). Contributions of bedrock groundwater to the upscaling of storm-runoff generation processes in weathered granitic headwater catchments. *Hydrological Processes, 29*(6), 1535-1548. https://doi.org/10.1002/hyp.10279

Iwasaki, K., Nagasaka, Y., & Nagasaka, A. (2021). Geological Effects on the Scaling Relationships of Groundwater Contributions in Forested Watersheds. *Water Resources Research, 57*(7), e2021WR029641. https://doi.org/10.1029/2021WR029641

Jitousono, T., Shimokawa, E., & Teramoto, Y. (2006). Potential site prediction of deep-seated landslide on the western flank of Mt. Yahazu-dake, Izumi City, Kagoshima Prefecture, Japan. *Sabo Gakkaishi, 59*(2), 5-12. https://doi.org/10.11475/sabo1973.59.2_5

Kanno, Y., Vokoun, J. C., & Letcher, B. H. (2014). Paired stream–air temperature measurements reveal fine-scale thermal heterogeneity within headwater brook trout stream networks. *River Research and Applications, 30*(6), 745-755. https://doi.org/10.1002/rra.2677

Meyer, J. L., Strayer, D. L., Wallace, J. B., Eggert, S. L., Helfman, G. S., & Leonard, N. E. (2007). The Contribution of Headwater Streams to Biodiversity in River Networks. *JAWRA Journal of the American Water Resources Association, 43*(1), 86-103. https://doi.org/10.1111/j.1752-1688.2007.00008.x

Nakagawa, Y., Nakashima, T., & Mawatari, K. (2002). Change in River Water Chemistry as Affected by the Confluence of Forest Drainage Water in Dairy Farming Area on Hokkaido Island, Northern Japan. *Journal of Forest Research, 7*(3), 131-136. https://doi.org/10.1007/BF02762601

Nhu, V.-H., Rahmati, O., Falah, F., Shojaei, S., Al-Ansari, N., Shahabi, H., et al. (2020). Mapping of Groundwater Spring Potential in Karst Aquifer System Using Novel Ensemble Bivariate and Multivariate Models. *Water, 12*(4), 985. https://doi.org/10.3390/w12040985

Niwa, H. (2022). Comparison of the accuracy of two UAV-mounted uncooled thermal infrared sensors in predicting river water temperature. *River Research and Applications*. https://doi.org/10.1002/rra.4027

Osanai, H., Sakō, S., Matsui, K., & Matsushita, K. (1968). *Explanatory text of the geological map of Japan, scale 1: 50000, Nishitappu*. Retrieved from

Rautio, A., Kivimäki, A. L., Korkka-Niemi, K., Nygård, M., Salonen, V. P., Lahti, K., & Vahtera, H. (2015). Vulnerability of groundwater resources to interaction with river water in a boreal catchment. *Hydrology and Earth System Sciences, 19*(7), 3015-3032. https://doi.org/10.5194/hess-19-3015-2015

Redder, B. W., Kennedy, C. D., Buda, A. R., Folmar, G., & Boyer, E. W. (2021). Groundwater contributions of flow and nitrogen in a headwater agricultural watershed. *Hydrological Processes, 35*(5), e14179. https://doi.org/10.1002/hyp.14179

Richards, G., Gilmore, T. E., Mittelstet, A. R., Messer, T. L., & Snow, D. D. (2021). Baseflow nitrate dynamics within nested watersheds of an agricultural stream in Nebraska, USA.

Agriculture, Ecosystems & Environment, 308, 107223. https://doi.org/10.1016/j.agee.2020.107223

Roesky, B., & Hayashi, M. (2022). Effects of lake-groundwater interaction on the thermal regime of a sub-alpine headwater stream. *Hydrological Processes, 36*(2), e14501. https://doi.org/10.1002/hyp.14501

Sakai, M., Iwabuchi, K., & Bauman, D. (2021). Unique habitat and macroinvertebrate assemblage structures in spring-fed stream: a comparison among clastic lowland tributaries and mainstreams in northern Japan. *Community Ecology, 22*(2), 193-202. https://doi.org/10.1007/s42974-021-00048-5

Schuetz, T., & Weiler, M. (2011). Quantification of localized groundwater inflow into streams using ground-based infrared thermography. *Geophysical Research Letters, 38*(3). https://doi.org/10.1029/2010GL046198

Tague, C., Farrell, M., Grant, G., Lewis, S., & Rey, S. (2007). Hydrogeologic controls on summer stream temperatures in the McKenzie River basin, Oregon. *Hydrological Processes, 21*(24), 3288-3300. https://doi.org/10.1002/hyp.6538

Takada, M., Mishima, Y., Kitagawa, R., & Mikami, H. (2009). Large scale evaluation of potential for Nitrate pollution in groundwater. *Report of Hokkaido Institute of Environmental Sciences, 35*, 21-26 (in Japanese with English summary).

Thompson, T. J., Briggs, M. A., Phillips, P. J., Blazer, V. S., Smalling, K. L., Kolpin, D. W., & Wagner, T. (2021). Groundwater discharges as a source of phytoestrogens and other agriculturally derived contaminants to streams. *Science of The Total Environment, 755*, 142873. https://doi.org/10.1016/j.scitotenv.2020.142873

Tokuni, M., Owari, T., Hirata, M., Suzuki, M., Takahashi, K., Kasahara, H., & Shibano, H. (2016). Positioning accuracy of mapping-and consumer-grade global navigation satellite system (GNSS) receivers in a forest environment. *Bulletin of The University of Tokyo Forests, 134*, 29-40 (in Japanese with English summary).

Ushijima, K., Ishii, A., Fukui, J.-i., & Matsumura, H. (2018). Feasibility of community based water management system on the basis of field study. *Journal of Japan Society of Civil Engineers, Ser. G (Environmental Research), 74*(7), III_143-III_152 (in Japanese with English summary). https://doi.org/10.2208/jscejer.74.III_143

Wagener, T., Dadson, S. J., Hannah, D. M., Coxon, G., Beven, K., Bloomfield, J. P., et al. (2021). Knowledge gaps in our perceptual model of Great Britain's hydrology. *Hydrological Processes, 35*(7), e14288. https://doi.org/10.1002/hyp.14288

Weatherill, J., Krause, S., Voyce, K., Drijfhout, F., Levy, A., & Cassidy, N. (2014). Nested monitoring approaches to delineate groundwater trichloroethene discharge to a UK lowland stream at multiple spatial scales. *Journal of Contaminant Hydrology, 158*, 38-54. https://doi.org/10.1016/j.jconhyd.2013.12.001

Wilbur, N. M., O'Sullivan, A. M., MacQuarrie, K. T. B., Linnansaari, T., & Curry, R. A. (2020). Characterizing physical habitat preferences and thermal refuge occupancy of brook trout (Salvelinus fontinalis) and Atlantic salmon (Salmo salar) at high river temperatures. *River Research and Applications, 36*(5), 769-783. https://doi.org/10.1002/rra.3570

Wing, M. G. (2008). Keeping Pace with Global Positioning System Technology in the Forest. *Journal of Forestry, 106*(6), 332-338. https://doi.org/10.1093/jof/106.6.332

Woli, K. P., Nagumo, T., Kuramochi, K., & Hatano, R. (2004). Evaluating river water quality through land use analysis and N budget approaches in livestock farming areas. *Science of The Total Environment, 329*(1), 61-74. https://doi.org/10.1016/j.scitotenv.2004.03.006

Water Resources Research

Supporting Information for

Thermal video recording while walking: A simple method for mapping groundwater discharge points along forested headwater streams

Kenta Iwasaki[1,2], Keitaro Fukushima[3,4], Yu Nagasaka[5], Nobuo Ishiyama[5], Masaru Sakai[6], and Akiko Nagasaka[5]

[1]Doto Station, Forestry Research Institute, Hokkaido Research Organization, Nishi5-sen 39-1, Shintoku, Hokkaido 081-0038, Japan.

[2]Present address: Center for Forest Damage and Risk Management, Forestry and Forest Products Research Institute, 1 Matsunosato, Tsukuba, Ibaraki 305-8687, Japan.

[3]Center for Ecological Research, Kyoto University, 2-509-3, Hirano, Otsu, Shiga, 520-2113, Japan

[4]Present address: Cluster of Agricultural Sciences, Faculty of Food and Agricultural Sciences, Fukushima University, 1 Kanayagawa, Fukushima, 960-1296, Japan

[5]Forestry Research Institute, Hokkaido Research Organization, Higashiyama, Koshunai, Bibai, Hokkaido 079-0198, Japan.

[6]Fukushima Regional Collaborative Research Center, National Institute for Environmental Studies, Japan, 10-2 Fukasaku, Miharu, Tamura District, Fukushima, 963-7700, Japan

Contents of this file

Introduction

This supporting information provides extra data, including a photograph of the equipment, a comparison between the RGB and thermal images, all minimum temperature data, the relationship between the tentative and actual temperatures, fluctuations in the stream water temperature during the survey period, and details of the hierarchical cluster analysis (HCA) results.

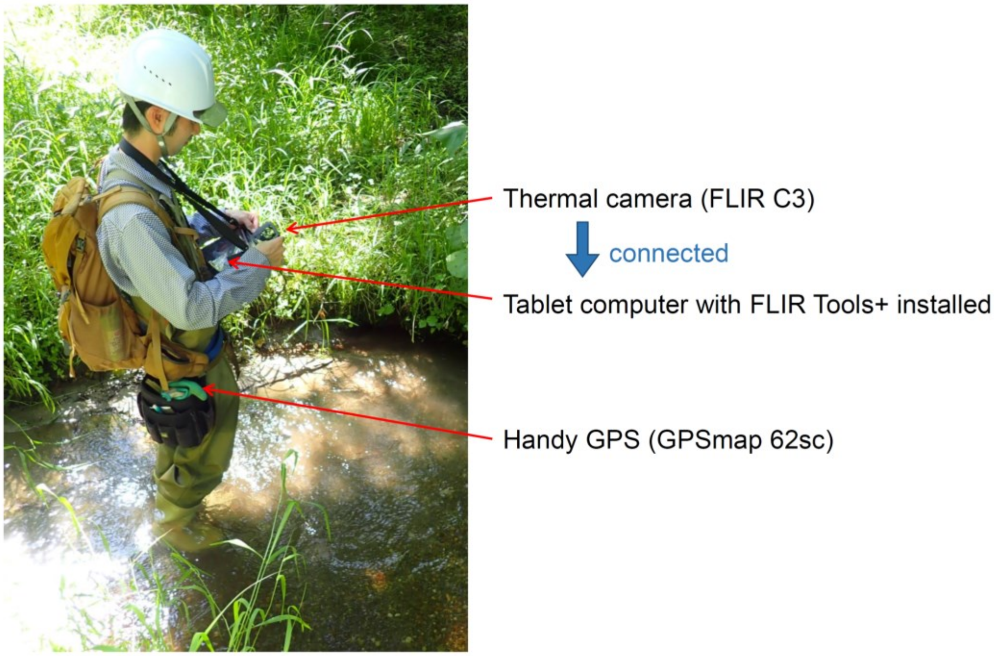

Figure S1. Photograph of the equipment used in the survey.

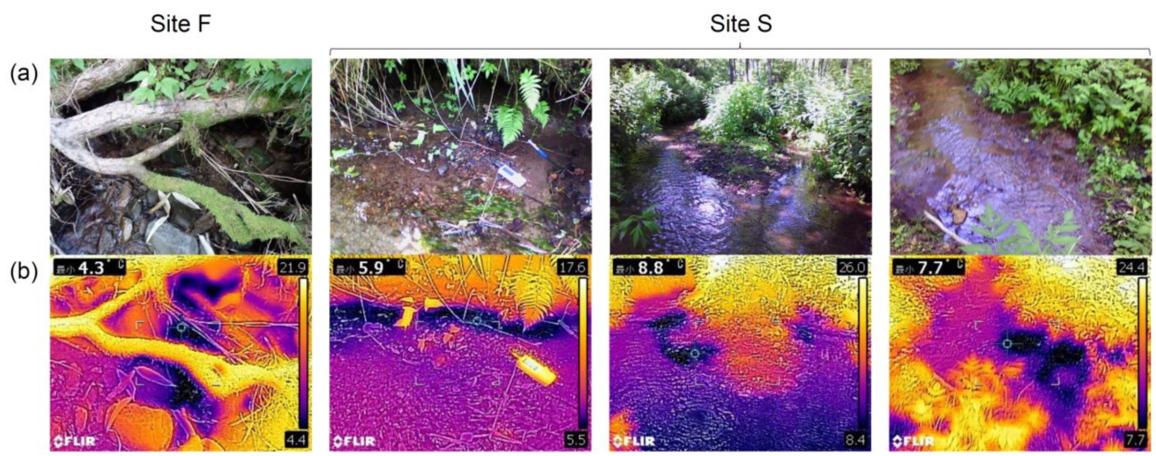

Figure S2. (a) RGB and (b) thermal images of the stream.

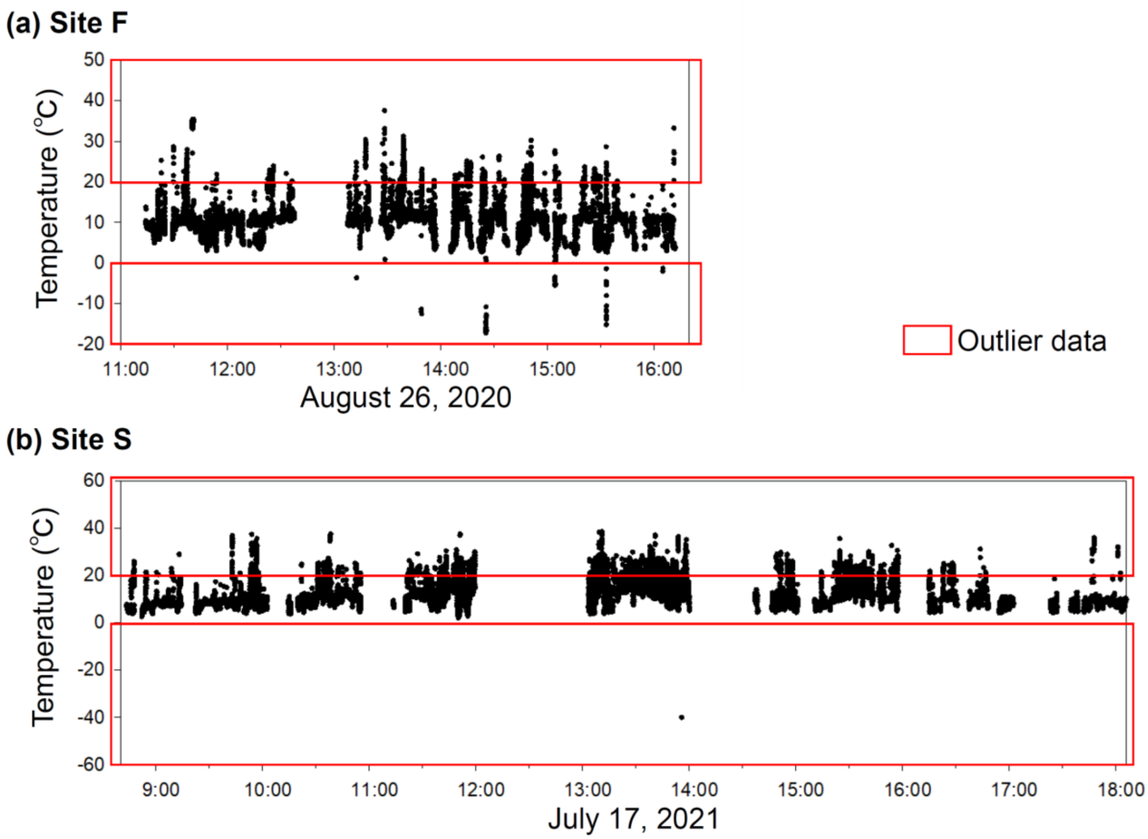

Figure S3. All minimum temperature data recorded at (a) Site F and (b) Site S.

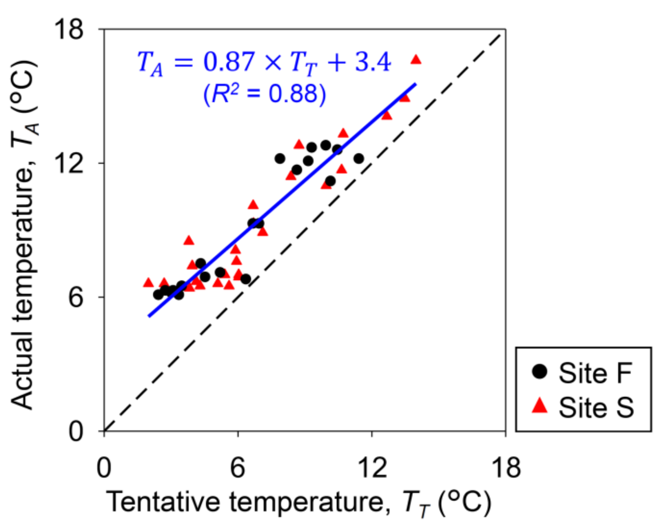

Figure S4. Relationship between the tentative temperature from thermal videos and actual temperature from a portable meter.

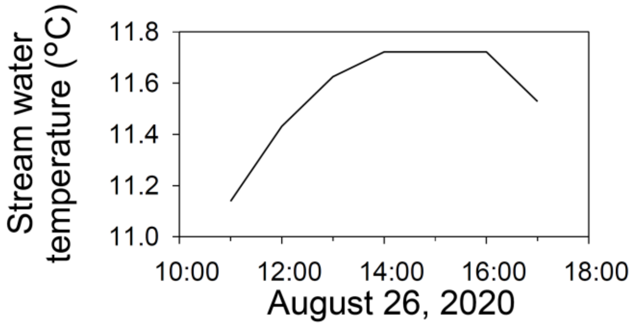

Figure S5. Fluctuations in the stream water temperature during the survey period at Site F.

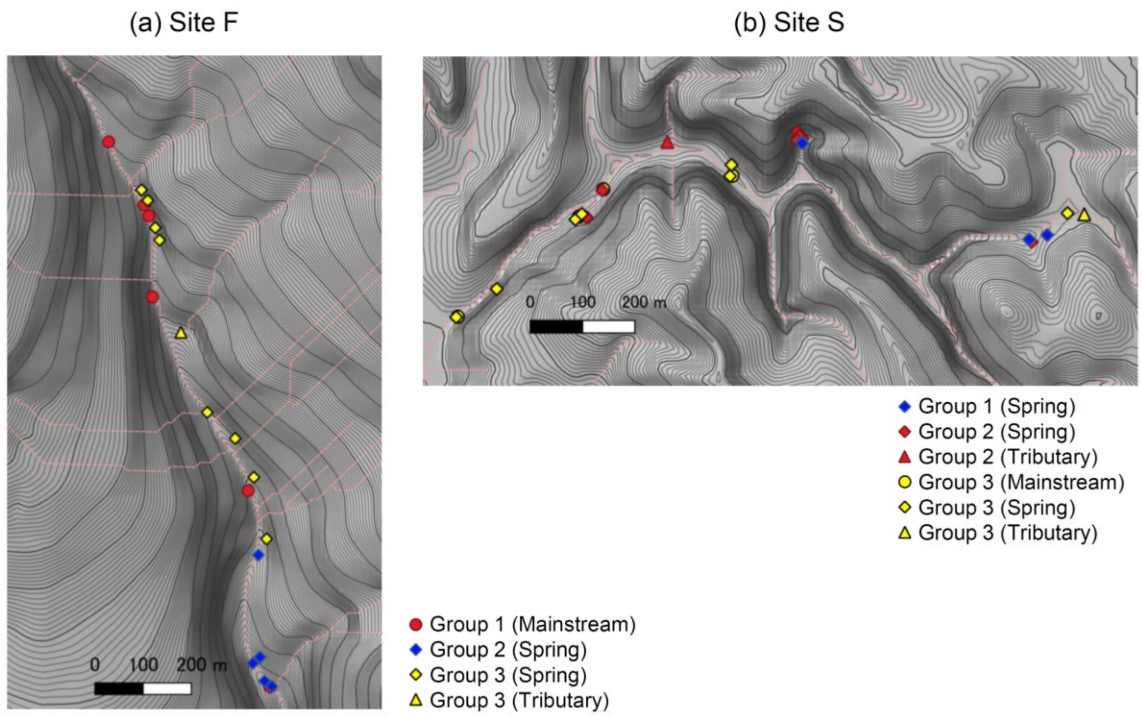

Figure S6. Sampling locations of each group at (a) Site F and (b) Site S.

Table S1. Mean water chemistry of the stream and spring samples in groups determined from HCA.

Group	EC (µS/cm)	pH	Solute concentrations (µmol/L)							
			Na^+	K^+	Mg^{2+}	Ca^{2+}	Cl^-	NO_3^-	SO_4^{2-}	PO_4^{3-}
Site F										
1	54.9 a	7.40 a	136 a	23 a	44 a	119 a	46 a	7 a	20 a	-
2	69.2 b	6.71 b	167 b	28 b	58 b	163 b	53 b	4 b	27 b	-
3	66.6 b	7.36 a	160 b	22 a	55 b	145 c	54 b	7 a	25 b	-
Site S										
1	168.5 a	6.62 a	417 a	58 a	162 a	423 a	235 a	100 a	28 a	0.99 a
2	70.3 b	7.06 b	256 b	41 b	51 b	137 b	78 b	19 b	20 b	0.78 a
3	117.1 c	7.10 b	335 c	48 c	106 c	270 c	139 c	64 c	18 b	0.98 a

Values not sharing the same letter are significantly different (Tukey-Kramer, $p < 0.05$).

Table S2. Mean water temperature and elevation of spring samples in groups determined from HCA.

Group	Water temperature (°C)		Elevation (m)
	From meter	From thermal video	
Site F			
2	7.46	7.38	752.20
3	7.29	7.68	809.49
Site S			
1	6.78	7.04	85.64
2	10.71	10.46	78.47
3	6.89	7.46	71.03